Electronic Supplementary Information for:

Discovery Of An Orexin Receptor Positive Potentiator

Jiyong Lee[1,3], M. Muralidhar Reddy and Thomas Kodadek[2*]

[1]Division of Translational Research, Departments of Internal Medicine and Molecular Biology, University of Texas Southwestern Medical Center, 5323 Harry Hines Blvd. Dallas, TX 75390 (USA).

[2]Departments of Chemistry & Cancer Biology, The Scripps Research Institute, Scripps Florida, 130 Scripps Way, Jupiter, FL 33458 (USA).

[3]Current Address: Department of Chemistry, The Scripps Research Institute, La Jolla, CA 92037 (USA).

[*] To whom correspondence should be addressed. E-mail: Kodadek@scripps.edu

Supporting Figures and Table

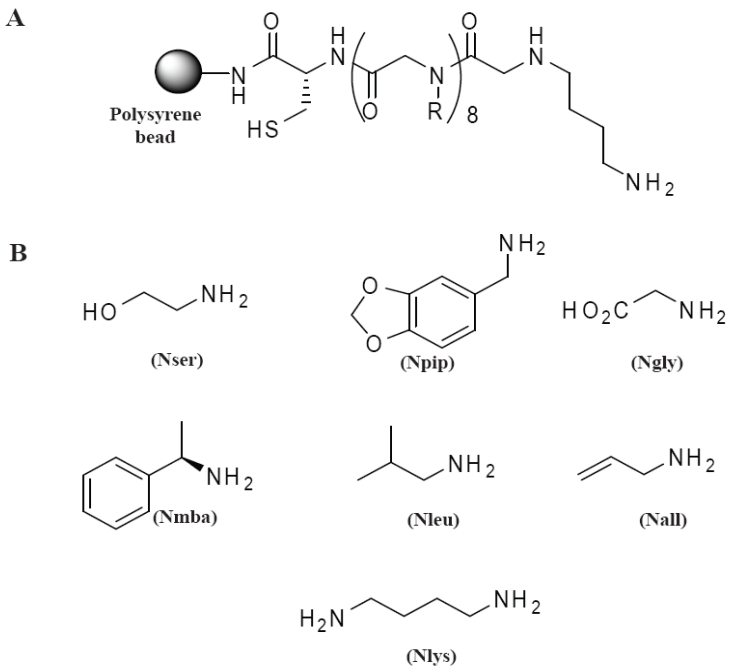

Fig. S1 The peptoid library used in this study. (A) General structure of peptoid library. (B) Amines used for the preparation of the library. In brackets included the corresponding nomenclature of the peptoid residues.

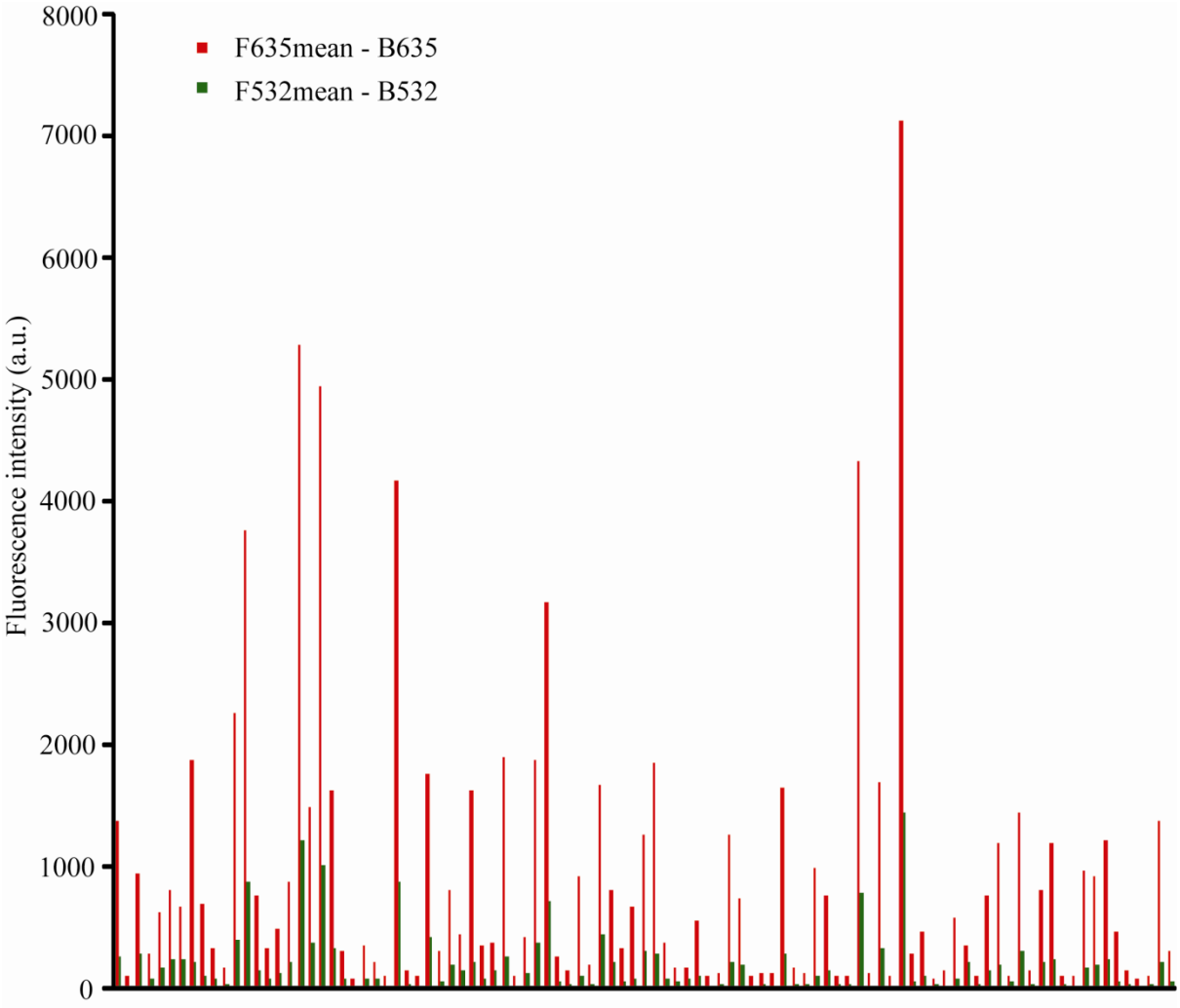

Fig. S2 Background-subtracted fluorescence emission intensities with 635nm and 532 nm (excitation wavelengths).

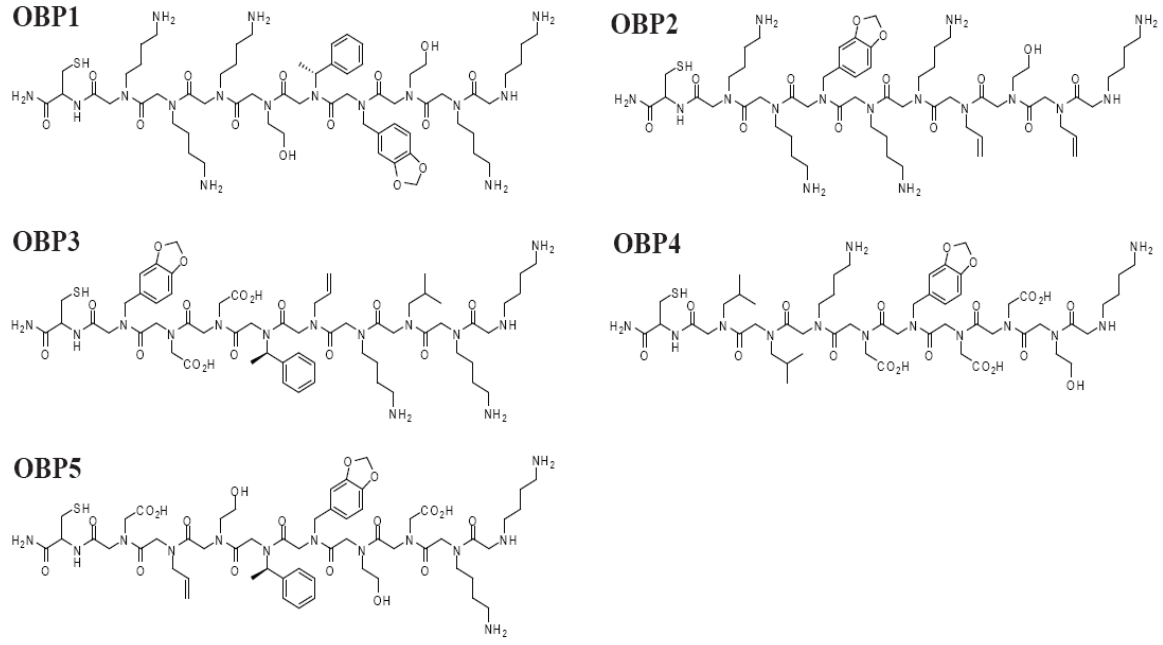

Fig. S3 Chemical structures of hit peptoids (OBPs).

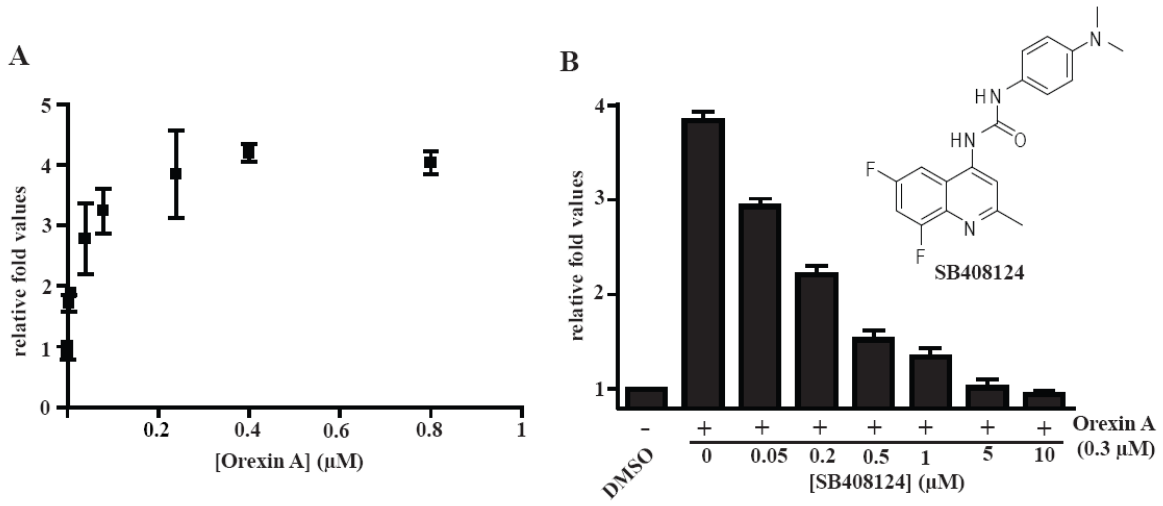

Fig. S4 A reporter gene assay monitoring OXR1 activation by orexin A. **(A)** Orexin A induced a dose-dependent increase of cAMP production. **(B)** The OXR1 selective antagonist, SB408124 blocks orexin-induced cAMP production. Error bars represent the standard deviation of the mean from triplicate experiments.

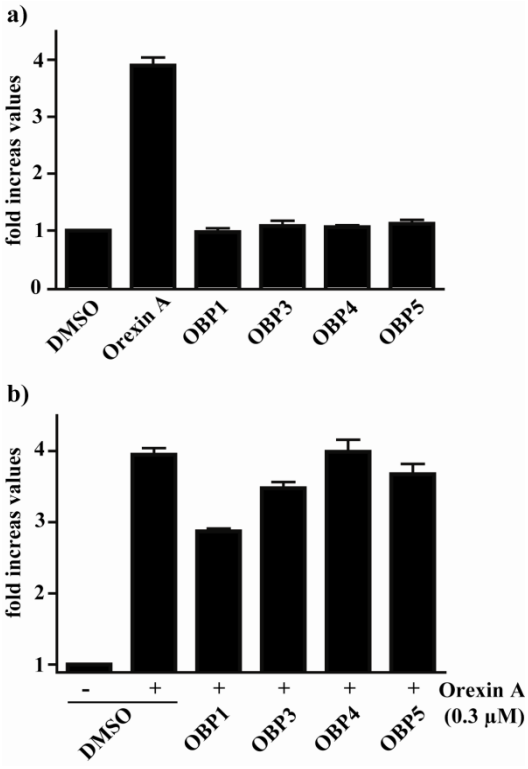

Fig. S5 Effects of hit peptoids on human OXR1 function. Hit peptoids (OBPs) were tested for their agonist (a) or antagonist (b) activities. Error bars represent the standard deviation of the mean from triplicate experiments.

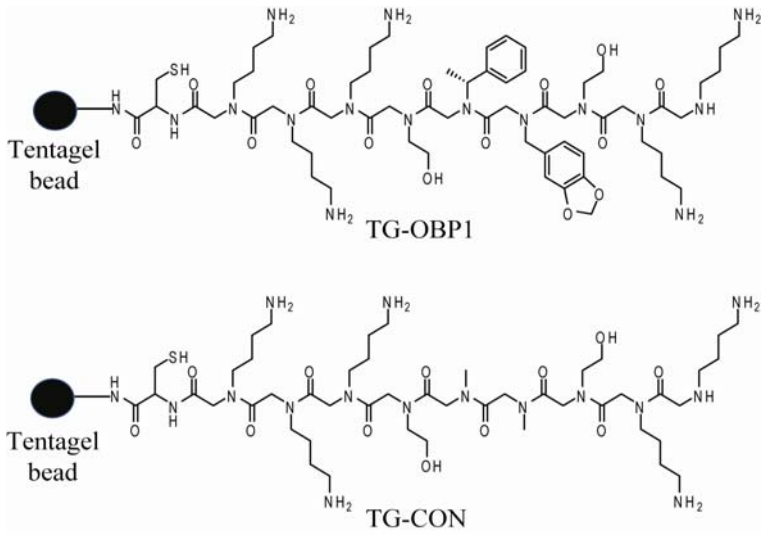

Fig. S6 Chemical structure of TG-OBP1 and TG-CON.

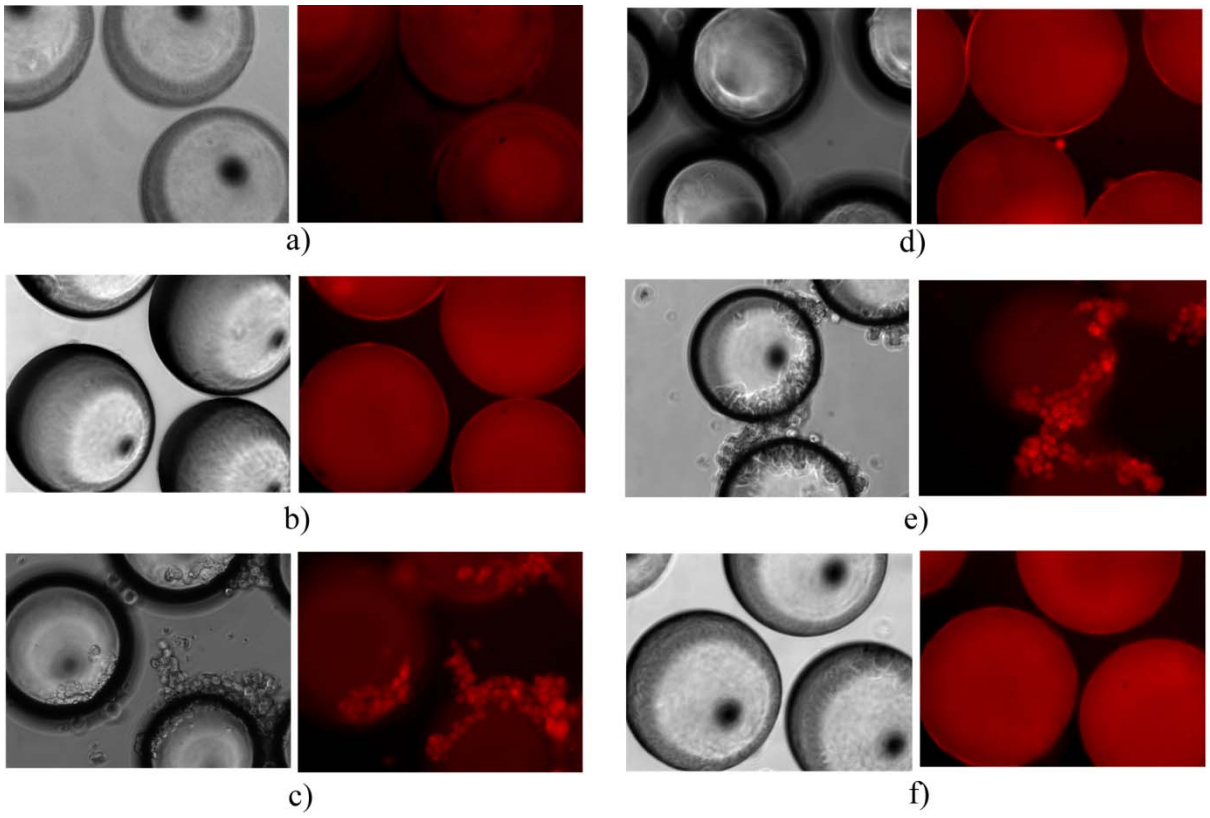

Fig. S7 Bead-binding assay. Peptoids on Tentagel beads were incubated with Syto60-stained HEK293/hOXR1 or HEK293 in conditions indicated below and visualized under light (left) / fluorescence microscopy (Cy5-channel, right). a) TG + HEK293/hOXR1, b) TG-OBP1 + HEK293, c) TG-OBP1 + HEK293/hOXR1, d) TG-CON + HEK293/hOXR1, e) TG-OBP1 + HEK293/hOXR1 with free orexin A (10 μM), f) TG-OBP1 + HEK293/hOXR1 with free OBP1 (5 mM). TG: Tentagel beads, TG-OBP1: Tentagel beads displaying OBP1, TG-CON: Tentagel beads displaying OBP1 in which side chains of Nmba and Npip were replaced with methyl groups.

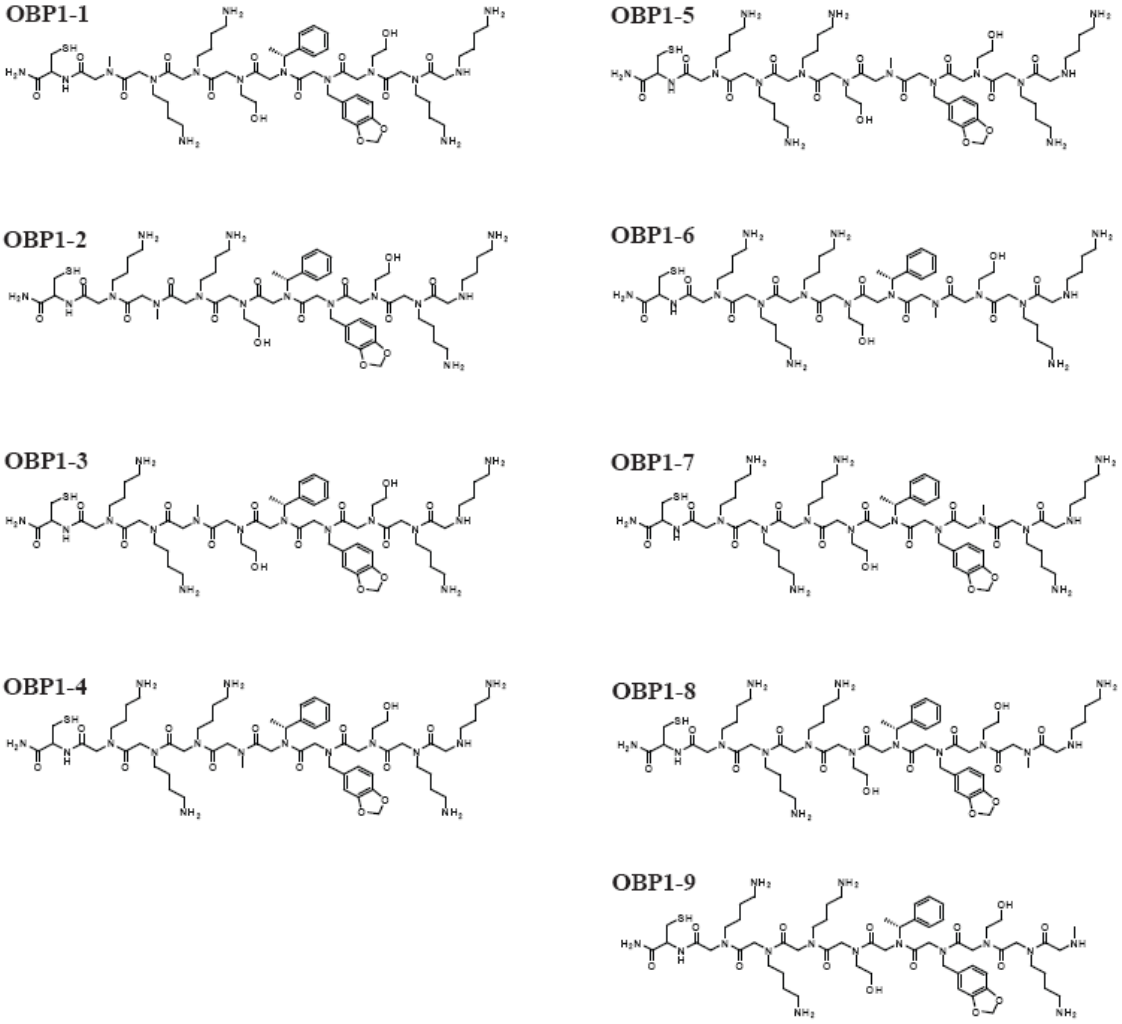

Fig. S8 Chemical structures of OBP1-N, sarcosine derivatives.

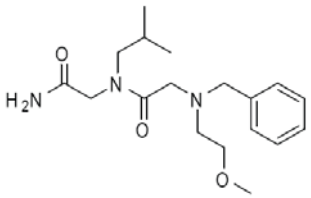

Fig. S9 Chemical structure of CON.

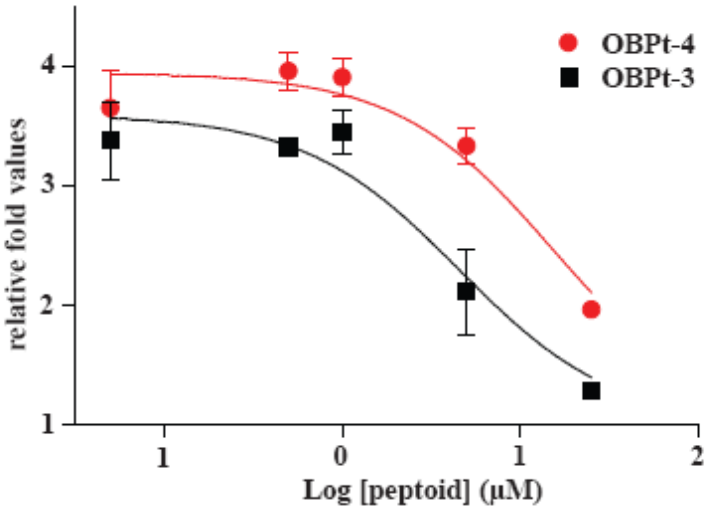

Fig. S10 Antagonist activities of OBPt-3 and OBPt-4. Error bars represent the standard deviation of the mean from triplicate experiments.

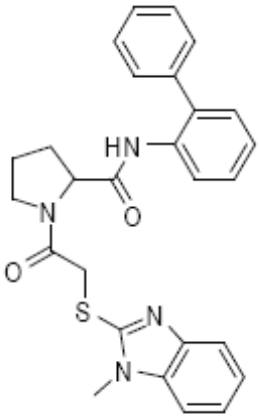

Fig. S11 Chemical structure of proline bis-amide.

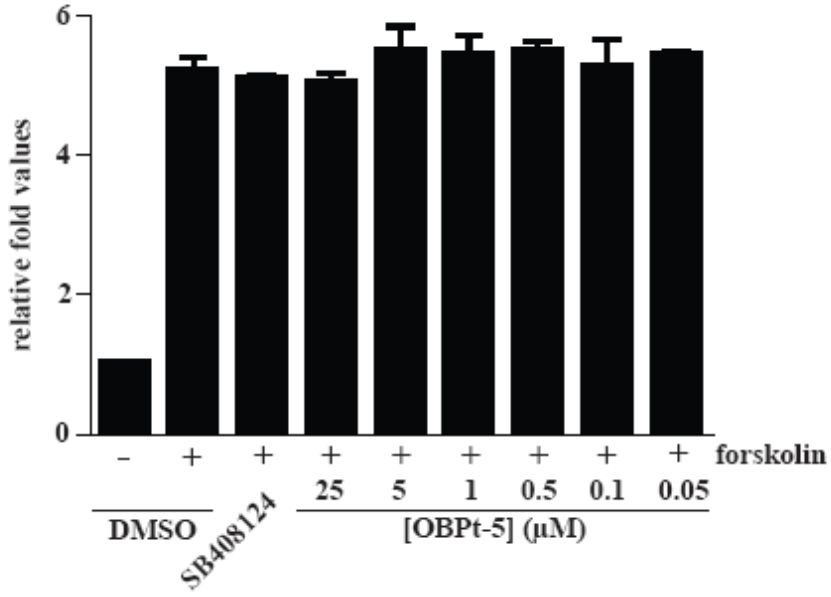

Fig. S12 Effect of OBPt-5 on forskolin (fsk)-induced cAMP production in HEK293 cells. Error bars represent the standard deviation of the mean from triplicate experiments.

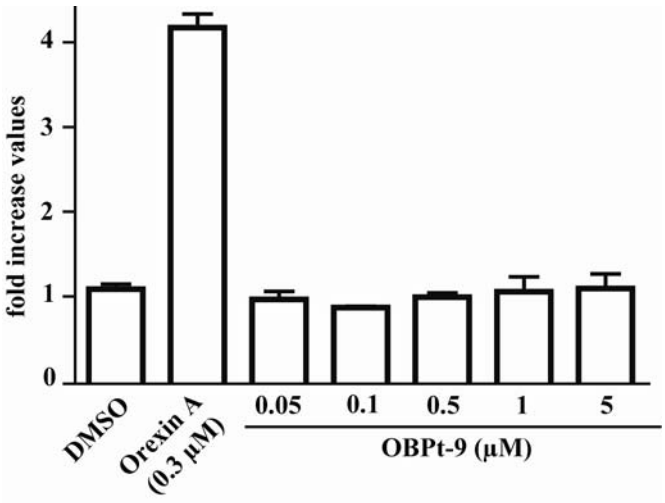

Fig. S13 Effect of OBPt-9 in the absence of orexin A on cAMP level of OXR1 expressing cells. HEK293/hOX1R cells were transfected with pGL3-3 × CRE-TATA and pRLuc for 24 hr. After starvation for 4 hr, DMSO, Orexin A, or increasing concentrations of OBPt-9 were added to cells. After 6 hr, cAMP elevation of cells was monitored by measuring luciferase activity of lysates. Error bars represent the standard deviation of the mean from triplicate experiments.

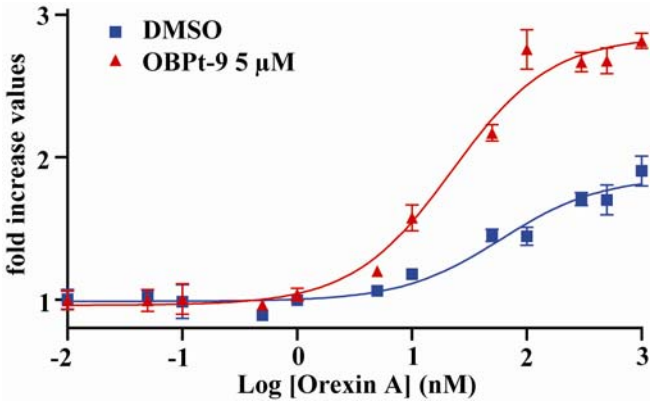

Fig.S14 Concentration-response curves of orexin A on cAMP elevation of OXR2 expressing cells in the presence or absence of OBPt-9. Error bars represent the standard deviation of the mean from triplicate experiments.

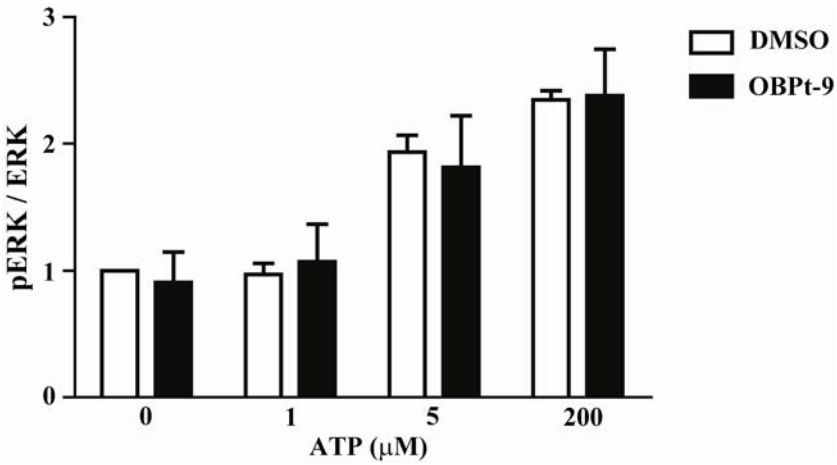

Fig. S15 Effect of OBPt-9 on P2 receptor-mediated ERK phosphorylation. Serum-starved HEK293 cells were treated with DMSO or OBPt-9 (5 μM) for 20 min. Then the cells were incubated with increasing concentration of ATP for 10 min. ERK phosphorylation was detected by Western analysis. Error bars represent the standard deviation of the mean from triplicate experiments.

Compound	Mass expected ($[M+H]^+$)	Mass found ($[M+H]^+$)
OBP1	1315.7	1315.8
OBP2	1247.7	1247.8
OBP3	1297.6	1297.7
OBP4	1240.5	1240.6
OBP5	1258.5	1258.6
OBP1-1	1258.6	1258.7
OBP1-2	1258.6	1258.7
OBP1-3	1258.6	1258.7
OBP1-4	1258.7	1285.8
OBP1-5	1225.7	1225.7
OBP1-6	1195.7	1195.8
OBP1-7	1285.7	1285.8
OBP1-8	1258.6	1258.7
OBP1-9	1258.6	1258.7
OBPt	370.1	370.2
OBPt-1	460.2	460.2
OBPt-2	474.2	496.4 ($[M+Na]^+$)
OBPt-3	403.1	403.2
OBPt-4	474.2	474.6
OBPt-5	417.2	417.7
OBPt-6	417.2	417.7
OBPt-7	469.2	469.5
OBPt-8	447.2	447.6
OBPt-9	476.2	476.5
CON	336.2	336.3

Table S1. MALDI-TOF/MS data.

MS/MS sequence analysis

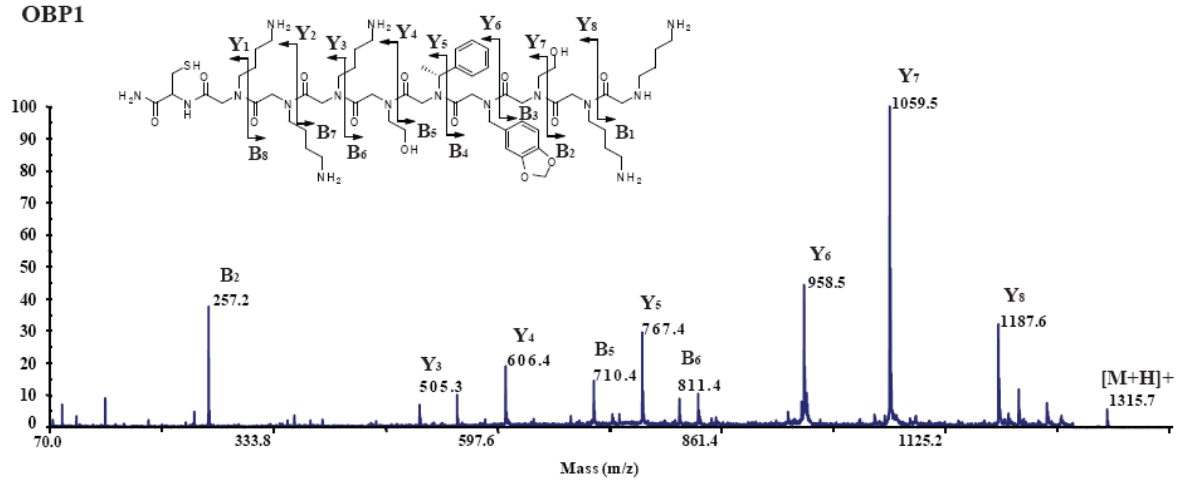

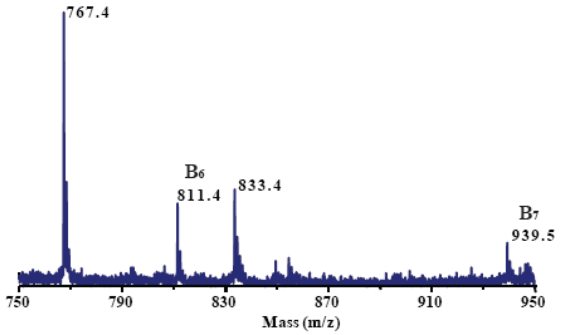

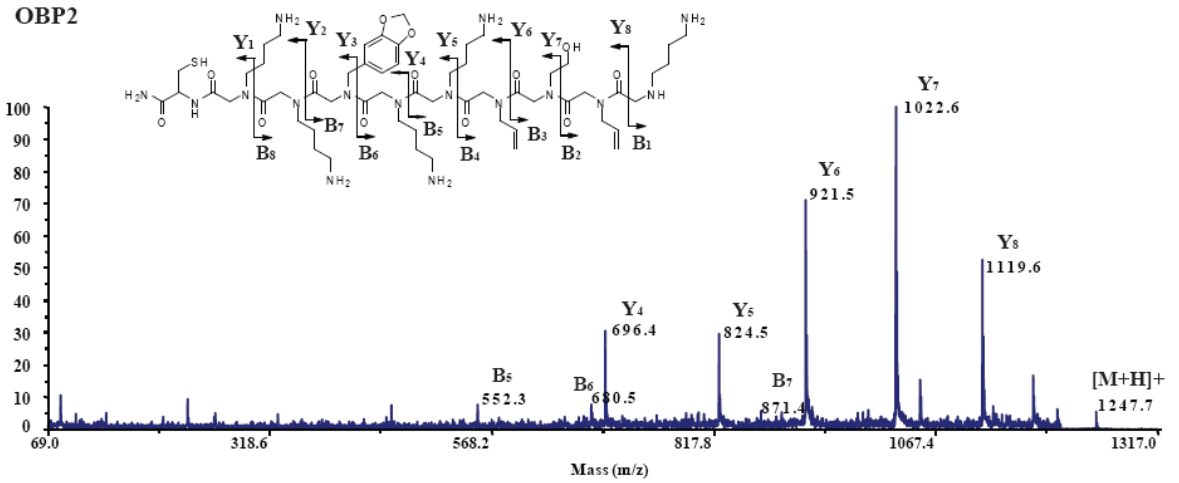

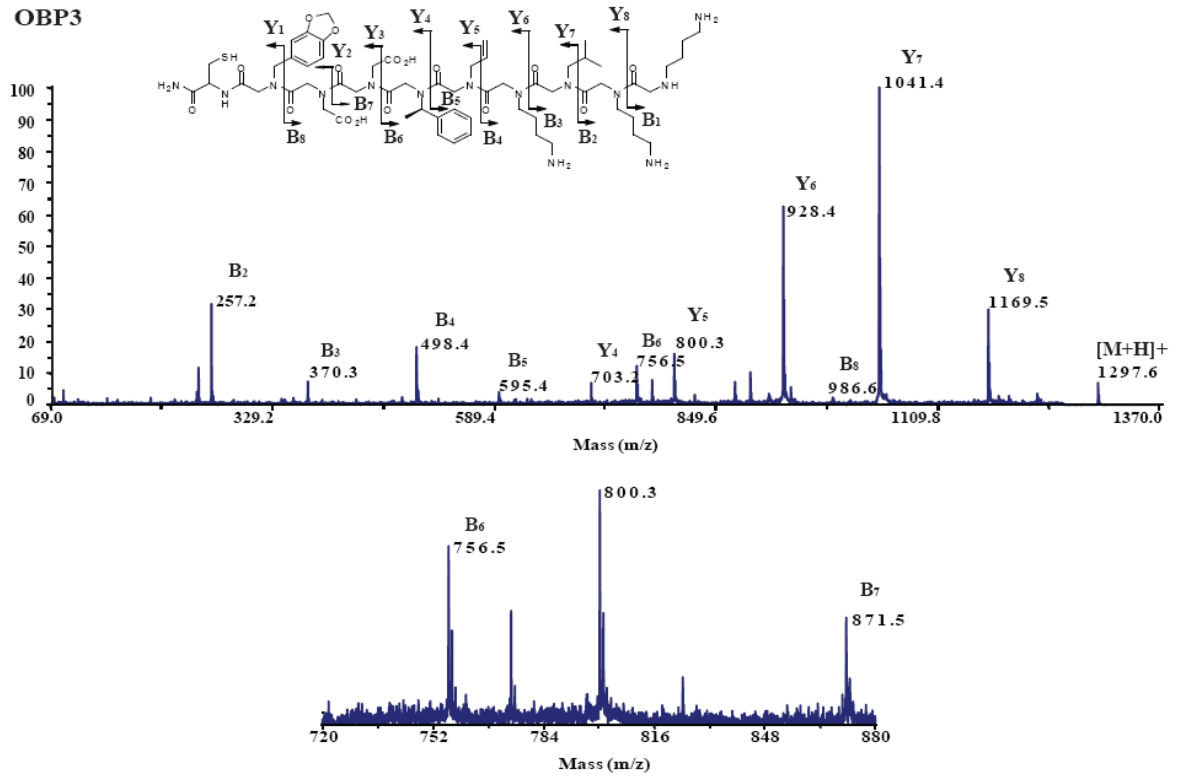
OBP3
Y1 Y2 Y3 Y4 Y5 Y6 Y7 Y8
B1 B2 B3 B4 B5 B6 B7 B8
Y7 1041.4
Y6 928.4
B2 257.2
Y8 1169.5
B4 498.4
Y5 800.3
B3 370.3
B6 756.5
Y4 703.3
B5 595.4
B8 986.6
[M+H]+ 1297.6
100
90
80
70
60
50
40
30
20
10
0
69.0
329.2
589.4
849.6
1109.8
1370.0
Mass (m/z)
800.3
B6 756.5
B7 871.5
720
752
784
816
848
880
Mass (m/z)

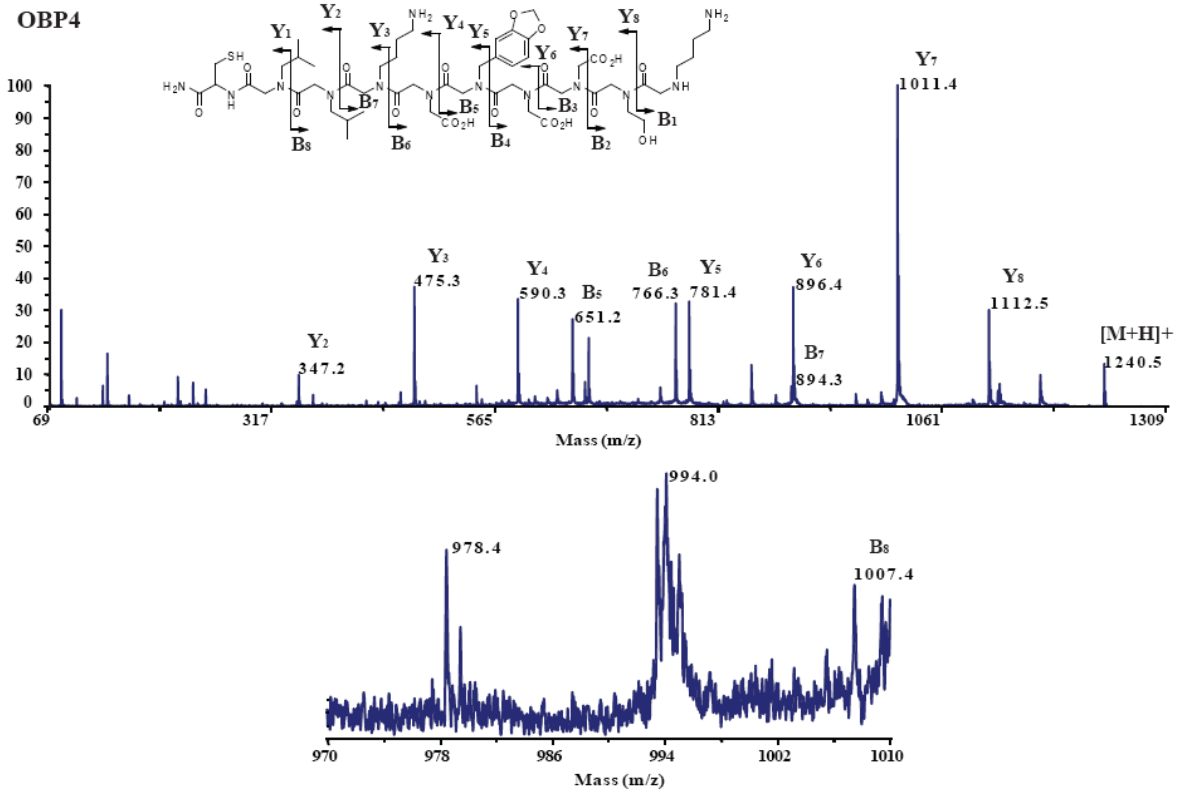
OBP4
Y1 Y2 Y3 Y4 Y5 Y6 Y7 Y8
B1 B2 B3 B4 B5 B6 B7 B8
Y7 1011.4
Y3 475.3
Y4 590.3
B5 651.2
B6 766.3
Y5 781.4
Y6 896.4
Y8 1112.5
Y2 347.2
B7 894.3
[M+H]+ 1240.5
100
90
80
70
60
50
40
30
20
10
0
69
317
565
813
1061
1309
Mass (m/z)
994.0
978.4
B8 1007.4
970
978
986
994
1002
1010
Mass (m/z)

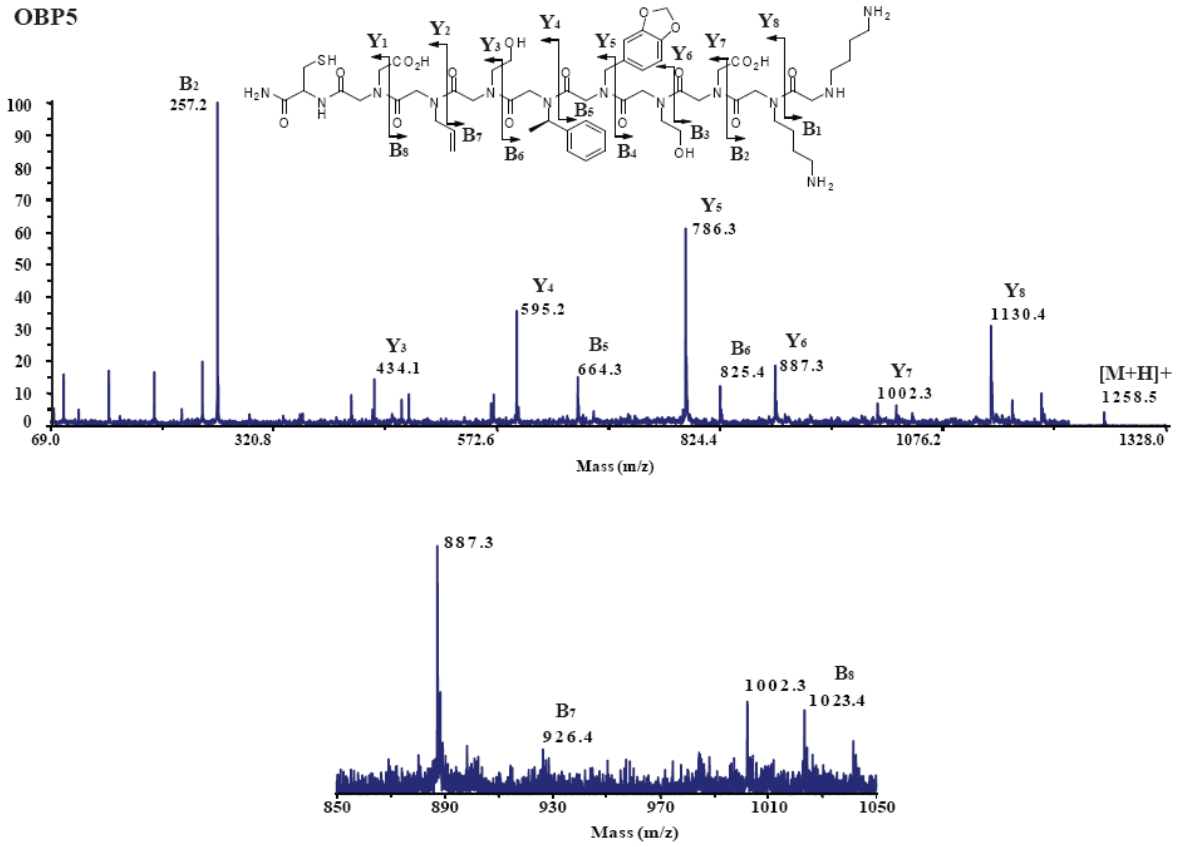
OBP5
B2
257.2
Y5
786.3
Y4
595.2
Y8
1130.4
Y3
434.1
B5
664.3
B6
825.4
Y6
887.3
Y7
1002.3
[M+H]+
1258.5
100
90
80
70
60
50
40
30
20
10
0
69.0
320.8
572.6
824.4
1076.2
1328.0
Mass (m/z)

887.3
B7
926.4
1002.3
B8
1023.4
850
890
930
970
1010
1050
Mass (m/z)